Proceedings of the ASME 2023
50th Annual Review of Progress in
Quantitative Nondestructive Evaluation
QNDE2023
July 24-27, 2023, Austin, Texas

QNDE2023-108620

LEARNING TENSOR REPRESENTATIONS TO IMPROVE QUALITY OF WAVEFIELD DATA

Harsha Vardhan Tetali[1], Joel B. Harley[1]*

[1]University of Florida, Gainesville, FL

ABSTRACT

Recent advancements in physics-informed machine learning have contributed to solving partial differential equations through means of a neural network. Following this, several physics-informed neural network works have followed to solve inverse problems arising in structural health monitoring. Other works involving physics-informed neural networks solve the wave equation with partial data and modeling wavefield data generator for efficient sound data generation. While a lot of work has been done to show that partial differential equations can be solved and identified using a neural network, little work has been done the same with more basic machine learning (ML) models. The advantage with basic ML models is that the parameters learned in a simpler model are both more interpretable and extensible. For applications such as ultrasonic nondestructive evaluation, this interpretability is essential for trustworthiness of the methods and characterization of the material system under test. In this work, we show an interpretable, physics-informed representation learning framework that can analyze data across multiple dimensions (e.g., two dimensions of space and one dimension of time). The algorithm comes with convergence guarantees. In addition, our algorithm provides interpretability of the learned model as the parameters correspond to the individual solutions extracted from data. We demonstrate how this algorithm functions with wavefield videos.

Keywords: Signal Processing, Machine Learning, Representation Learning, Optimization Theory, Denoising, Image and Video Quality Assessment

1. INTRODUCTION

Guided waves have gained attention in the realm of structural health monitoring due to their wide applicability and complex nature. Ultrasonic guided waves have proven valuable in detecting, locating, and characterizing damage within various physical structures [1–3]. Their ability to cover large areas with minimal attenuation has led to their implementation in a diverse array of structural systems, such as pipelines [2, 4–9], bridges [10, 11], concrete structures [12], steel cables [13–15], metal aircraft components [16, 17], and composite aircraft components [18–21]. To measure guided waves, researchers often utilize densely sampled wavefield imaging systems, such as scanning laser Doppler vibrometers [22]. Consequently, the development of efficient and accurate methods for processing and interpreting wavefield data has become an area of significant interest.

A recent advancement that has potential in improving the analysis of wavefields is physics-informed machine learning. Specifically, recent advancements in Physics-Informed Neural Networks (PINNs) [23] have revolutionized our ability to solve and identify partial differential equations (PDEs) using neural networks. This work has spurred a myriad of applications in SHM, such as identifying cracks through ultrasound imaging[24], structural identification through neural networks [25], and solving the wave-equation with partial data [26, 27]. While these black-box neural network models have shown promise, their complex nature often precludes interpretability and convergence guarantees of the optimization algorithm, which are crucial factors in establishing trustworthiness and reliability for practical applications. Additionally, these networks need a large collection of training data, significant computational power, and a long training time.

In this paper, we present an interpretable, physics-informed representation learning framework (based on [28–30]) capable of analyzing wavefield data across multiple dimensions (e.g., two dimensions of space and one dimension of time) while providing convergence guarantees for the optimization algorithm. The proposed method offers enhanced interpretability compared to traditional black-box neural networks, as the parameters in the learned model correspond to the individual solutions extracted from the data. The framework utilizes physics and data to produce required results and does not need additional data to train.

Furthermore, our framework enables the enhancement of wavefield quality using physics-informed representation learning. The intuition of wave propagation is encoded in the wave

*Corresponding author: joel.harley@ufl.edu

equation and dates back to Brooke Taylor [31], who discovered the wave equation through simple physical insight [32]. We leverage this mathematical intuition of the wave equation to enforce structure into a representation learning algorithm and learn noise-free representations that can eventually enhance the visual quality of the wavefield. This enhancement in resolution offers advantages for structural health monitoring like improving the reliability and accuracy of structural defects and the like.

We demonstrate the efficacy of our algorithm by showing an improvement in the quality of synthetic wavefield video data obtained from [33]. The wave data obtained from [33] has artifacts introduced by interpolating a low resolution video. In this paper, we show that these artifacts can be eliminated to provide a cleaner wavefield video.

2. WAVE-INFORMED REPRESENTATION LEARNING

In this section, we introduce wave-informed decompositions, an approach to extract noiseless and distortion-less reconstructions of a measured wavefield video, enabling a more accurate and efficient analysis of wave-based phenomena.

Wave-informed decompositions leverage the power of representation learning to disentangle the individual velocity components of a wavefield by enforcing a discretized version of the wave equation. This approach ensures that the extracted representations are both physically meaningful and adhere to the underlying governing wave equation. We obtain the reconstruction by recombining these representations.

To achieve this, we formulate an optimization problem that seeks to minimize the discrepancy between the original wavefield and the reconstructed wavefield obtained from the decomposition. This optimization framework captures the essential constraints derived from the discretized wave equation and ensures that the obtained representations are consistent with the mathematical physics of wave propagation.

Furthermore, we use an algorithm to tackle this optimization problem, which guarantees convergence to global optimality. This algorithm is interpretable and also best reconstructs the original wavefield, while remaining computationally tractable.

In the following sections, we will delve into the intricacies of wave-informed decompositions, detailing the discretized wave equation, the optimization problem formulation, and the proposed algorithm for achieving global optimality. Through these discussions, we aim to provide a comprehensive understanding of this technique and its potential applications in various domains involving wave-based signals.

2.1 Discrete Wavefields as Tensors

Consider a continuous wavefield $f(x, y, t)$ on a finite structure for a finite time period. Consider for simplicity, $x \in [0, L_x]$, $y \in [0, L_y]$ and $t \in [0, T]$. Let N_x, N_y and N_t be points be sampled in each space dimension and time dimension respectively. The sampling periods in space and time are given by, $\Delta x = L_x/N_x$, $\Delta y = L_y/N_y$ and $\Delta t = T/N_t$. Consider the tensor $\mathbf{U} \in \mathbb{R}^{N_x \times N_y \times N_t}$, such that:

$$\mathbf{U}_{i_x, i_y, i_t} = f\left(i_x \Delta x, i_y \Delta y, i_t \Delta t\right). \tag{1}$$

Note that the tensor $\mathbf{F}$ represents a discretized version of the wave-field $f(x, y, t)$. In the decomposition algorithm we present, we consider vectorized versions of the tensors represented by $\mathrm{vec}(\mathbf{F})$.

2.2 Discrete Version of the Wave equation

The two (spatial) dimensional wave equation for a wave propagating at velocity c is given by:

$$\frac{\partial^2 u(x, y, t)}{\partial x^2} + \frac{\partial^2 u(x, y, t)}{\partial y^2} = \frac{1}{c^2} \frac{\partial^2 u(x, y, t)}{\partial t^2} \tag{2}$$

Assuming that $\mathbf{U}$ is the tensor corresponding to the wavefield $u(x, y, t)$, discretized version of the wave equation is:

$$\begin{aligned}(\boldsymbol{I}_t \otimes \boldsymbol{I}_2 \otimes \boldsymbol{L}_1 + \boldsymbol{I}_t \otimes \boldsymbol{L}_2 \otimes \boldsymbol{I}_1)\, \mathrm{vec}(\mathbf{U}) \\ = \frac{1}{c^2} (\boldsymbol{L}_t \otimes \boldsymbol{I}_2 \otimes \boldsymbol{I}_1)\, \mathrm{vec}(\mathbf{U})\end{aligned} \tag{3}$$

2.3 Formulating the Objective

Given the discretized wave data $\mathbf{Y} \in \mathbb{R}^{N_x \times N_y \times N_t}$, our goal is to decompose the tensor $\mathbf{Y}$ into a sum of tensors, each satisfying a discrete version of the wave equation. The idea behind the decomposition can be succinctly expressed through the following equation:

$$\mathbf{Y} = \mathbf{U}_1 + \mathbf{U}_2 + \cdots \mathbf{U}_m \tag{4}$$

where $\mathbf{U}_i$ for $i \in [m]$ must satisfy a discrete version of the wave equation. To leverage linear algebraic concepts and formulate the problem in terms of matrix factorization, it is often more convenient to vectorize (flatten) the tensors and work with vectors. For the matrix factorization formulation, we rewrite equation 4 in vector form as:

$$\boldsymbol{y} = \sum_{i=1}^{m} \boldsymbol{u}_i \tag{5}$$

where $\boldsymbol{y} = \mathrm{vec}(\mathbf{Y})$ and $\boldsymbol{u}_i = \mathrm{vec}(\mathbf{U}_i)$, for $i \in [m]$. Now, assuming each $\boldsymbol{u}_i = \boldsymbol{D}_i x_i$, with x_i being a scaling factor, we ultimately express our representation as $\boldsymbol{y} = \boldsymbol{D}\boldsymbol{x}$, where $\boldsymbol{D}$ contains $\boldsymbol{D}_i$ as its columns and $\boldsymbol{x}$ contains x_i for $i \in [m]$ as its elements. This constitutes the matrix factorization component of the objective function.

The original setup, without vectorizing, required $\mathbf{U}_i$ to satisfy a discrete version of the wave equation. This translates to having a similar assumption on $\boldsymbol{D}_i$ (since x_i are just scalars), albeit in a slightly different form. Let $\mathscr{W}_{c_i}(\boldsymbol{D}_i) = 0$ represent the discrete version of the wave equation with the wave velocity parameter c_i. To enforce structure from the wave equation, we can minimize $\min_{c_i} \left\|\mathscr{W}_{c_i}(\boldsymbol{D}_i)\right\|_2^2$ as part of the regularizer. Additionally, we aim to constrain the number of velocity modes to be minimal. We achieve this by adding the squared Frobenius norms of both $\boldsymbol{D}$ and $\boldsymbol{x}$. This is known to induce low-rank solutions in the product $\boldsymbol{D}\boldsymbol{x}$ due to connections with the variational form of the nuclear norm [34], [35], [36], [37]. We finally obtain the regularizer:

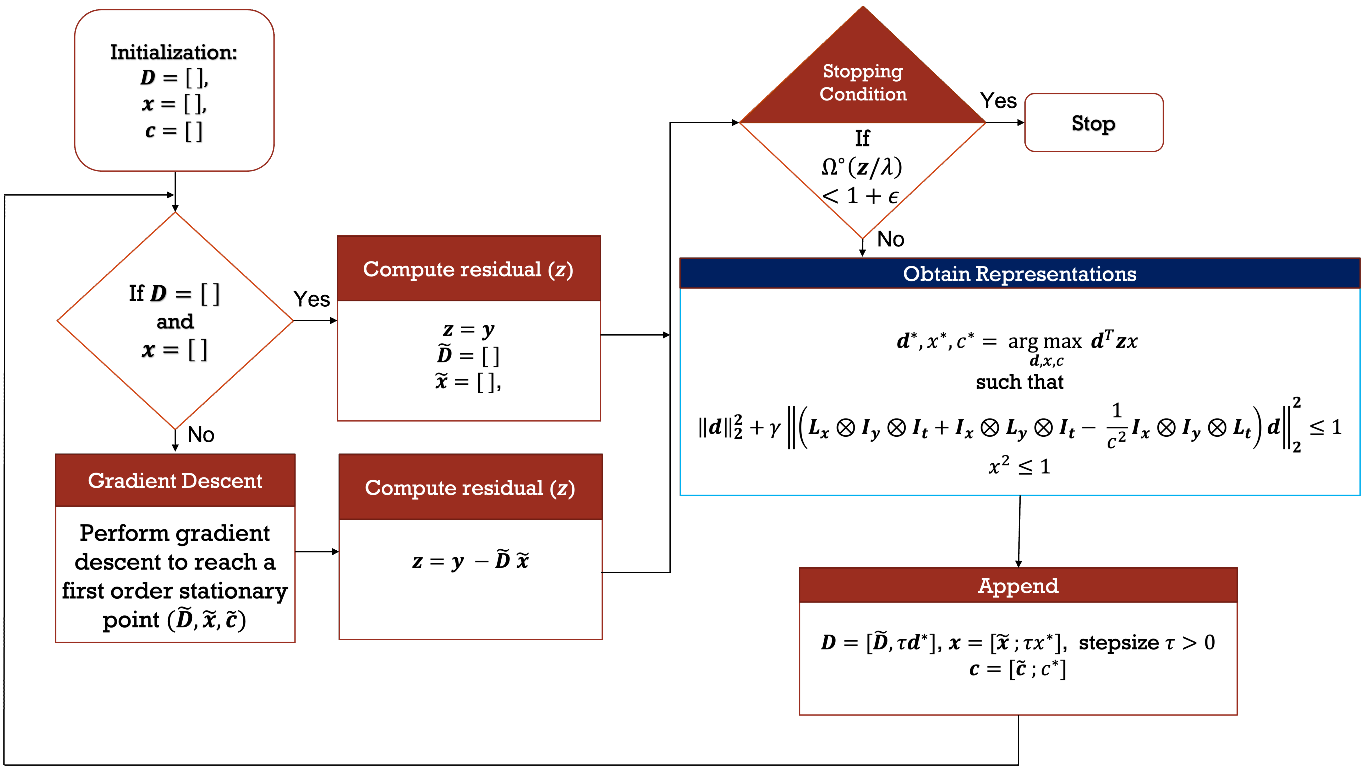

FIGURE 1: WAVE-INFORMED DECOMPOSITION FLOWCHART

$$\Theta(\boldsymbol{D}, \boldsymbol{x}) = \sum_{i=1}^{M} \bar{\theta}(\boldsymbol{D}_i, x_i) \tag{6}$$

where $\gamma > 0$ is a tunable parameter and $\bar{\theta}(\boldsymbol{D}_i, x_i) = \gamma \min_{c_i} \left\| \mathcal{W}_{c_i}(\boldsymbol{D}_i) \right\| + \|\boldsymbol{D}_i\|_2^2 + x_i^2$. The final optimization problem formulated is:

$$\min_{M} \min_{\boldsymbol{D},\boldsymbol{x},\boldsymbol{c}} \frac{1}{2} \|\boldsymbol{y} - \boldsymbol{D}\boldsymbol{x}\|_2^2 + \frac{\lambda}{2} \left(\sum_{i=1}^{M} \gamma \min_{c_i > 0} \|\mathcal{W}_{c_i}(\boldsymbol{D}_i)\|_2^2 + \|\boldsymbol{D}_i\|_2^2 + x_i^2 \right). \tag{7}$$

$\mathcal{W}_{c_i}(.)$ is a linear operator dependent on c_i and therefore we can have a matrix such that, $\mathcal{W}_{c_i}(\boldsymbol{v}) = \boldsymbol{A}_{c_i} \boldsymbol{v}$. For,

$$\boldsymbol{A}_c = \boldsymbol{L}_x \otimes \boldsymbol{I}_y \otimes \boldsymbol{I}_t + \boldsymbol{I}_x \otimes \boldsymbol{L}_y \otimes \boldsymbol{I}_t - \frac{1}{c^2} \boldsymbol{I}_x \otimes \boldsymbol{I}_y \otimes \boldsymbol{L}_t \tag{8}$$

and $\lambda > 0$ is the regularization weighting the term $\Theta(\boldsymbol{D}, \boldsymbol{x})$.

2.4 The Optimization Algorithm

Using a flowchart (see Fig. 1), we simply state the algorithm we use for solving this optimization, theoretical details can be found in [29, 36, 37]. The algorithm starts with an empty matrix $\boldsymbol{D}$ and an empty vector $\boldsymbol{x}$ and increase the number of columns of $\boldsymbol{D}$ by 1 and appropriately change the size of vector $\boldsymbol{x}$ in each iteration (see the block on *Obtaining Representations* in Fig 1 highlighted in blue, this step produces the column that needs to be appended). The algorithm stops close to global optimality due to the stopping condition $\Omega^\circ(z/\lambda) < 1 + \epsilon$ (see equation 9), which ensures the obtained $\boldsymbol{D}$ and $\boldsymbol{x}$ is $\mathcal{O}(\epsilon)$ close to the optimal solution ([37], Prop. 4) for a user chosen $\epsilon > 0$.

$$\Omega_\theta^\circ \left(\frac{z}{\lambda} \right) = \max_{\boldsymbol{d},x,c_i} \boldsymbol{d}^\top \left(\frac{z}{\lambda} \right) x$$
$$\text{s.t. } \|\boldsymbol{d}\|_2^2 + \gamma \, \|\boldsymbol{A}_c \boldsymbol{d}\|_2^2 \le 1, x^2 \le 1. \tag{9}$$

3. RESULTS

We use a data set of wave propagation from [33] to show a reconstruction result. Fig. 2 represents different time frames of the data set. The data set represents video of a waves propagating over a fluid medium. Each frame in the video is 343 ($= N_1$) pixels high and 434 ($= N_2$) wide. In Fig. 2, observe the distortions in the video frames introduced due to interpolation of a low-resolution wavefield video. This distortion is introduced due to the interpolation algorithm that does not respect wave behaviour while interpolating low resolution wavefield videos. We consider the first 100 time points in our reconstruction. Fig. 3 shows a reconstruction based on wave-informed decomposition algorithm. Observe that the waves are much smoother and clear and without distortions as compared to original (Fig. 2). We have the following empirically chosen values for running the algorithm for $\epsilon = 0.1$, $\gamma = 0.5(N_1/\pi)^2$ and $\lambda = 0.1$ (see [29, 30] for details about choice of parameter values).

The algorithm extracts relevant features, each of which are waves that propagate at a fixed velocity. The pixelated artifacts introduced due to low-resolution imaging are considered noise

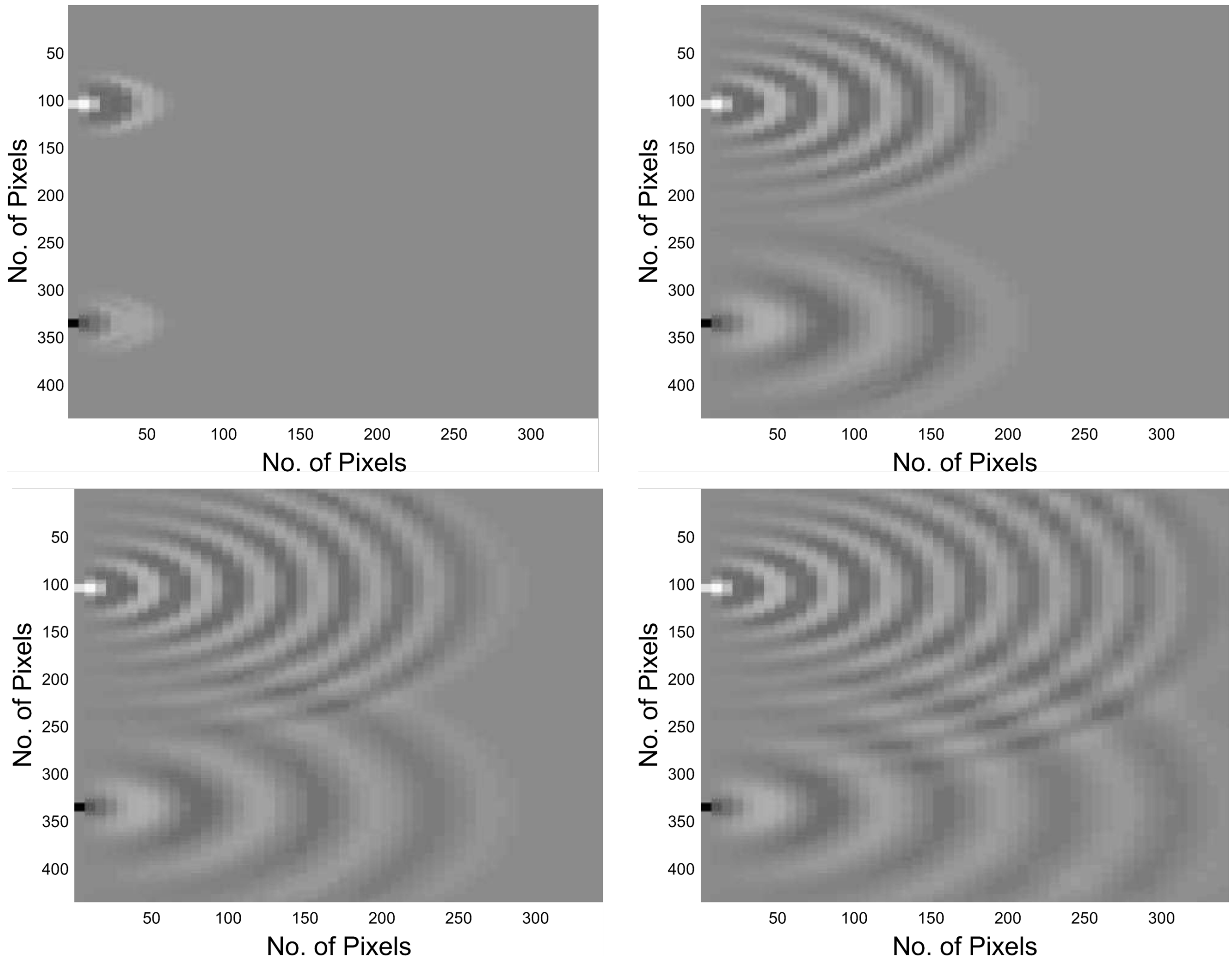

FIGURE 2: ORIGINAL VIDEO OF WAVES EMERGING FROM TWO DIFFERENT DROPLETS OF DIFFERENT MASSES FALLING ONTO A WATER SURFACE

(for the wave-informed algorithm) since pixelated images are non-smooth and do not minimize the wave equation (which needs the image to be as smooth as possible due to the computation of the second derivative). Thus, the non-smooth part of the image is not learned as the representation. The representations extracted by the algorithm are a good representative of the data and also follow the physics of waves resulting in representations that are smooth and hence give the visual perception of a clean and smooth wavefield (as in Fig. 3).

4. CONCLUSIONS AND FUTURE WORK

In this study, we have presented an interpretable, physics-informed representation learning framework for quantitative non-destructive evaluation, offering a robust and reliable alternative to traditional black-box neural networks. Our approach has demonstrated the ability to analyze data across multiple dimensions through a custom optimization process, while providing convergence guarantees and improved interpretability. Our framework has successfully demonstrated an improvement in the quality of wavefield imaged at a low resolution. This has potential benefits for structural health monitoring, such as improved defect detection and localization, enhanced resolution and sensitivity, and reduced data noise and artifacts. The wavefield reconstruction showcased in this work effectively eliminates distortions caused by interpolation of low-resolution wavefields, paving the way for more accurate and reliable assessments of structural integrity.

In future work, the development and implementation of appropriate image and video quality metrics will be crucial in quantifying the performance of our method. By measuring the image and video quality of reconstructed wavefields, we can further refine our framework and optimize its capabilities for various applications in the field of structural health monitoring. Additionally, we plan to explore the applicability of the interpretability of the proposed framework, demonstrating the isolation of different velocities and further solidifying its practical advantages.

Ultimately, this research lays the foundation for advancing the state-of-the-art in physics-informed representation learning and contributes to the ongoing pursuit of trustworthy, interpretable, and accurate methods for quantitative non-destructive evaluation.

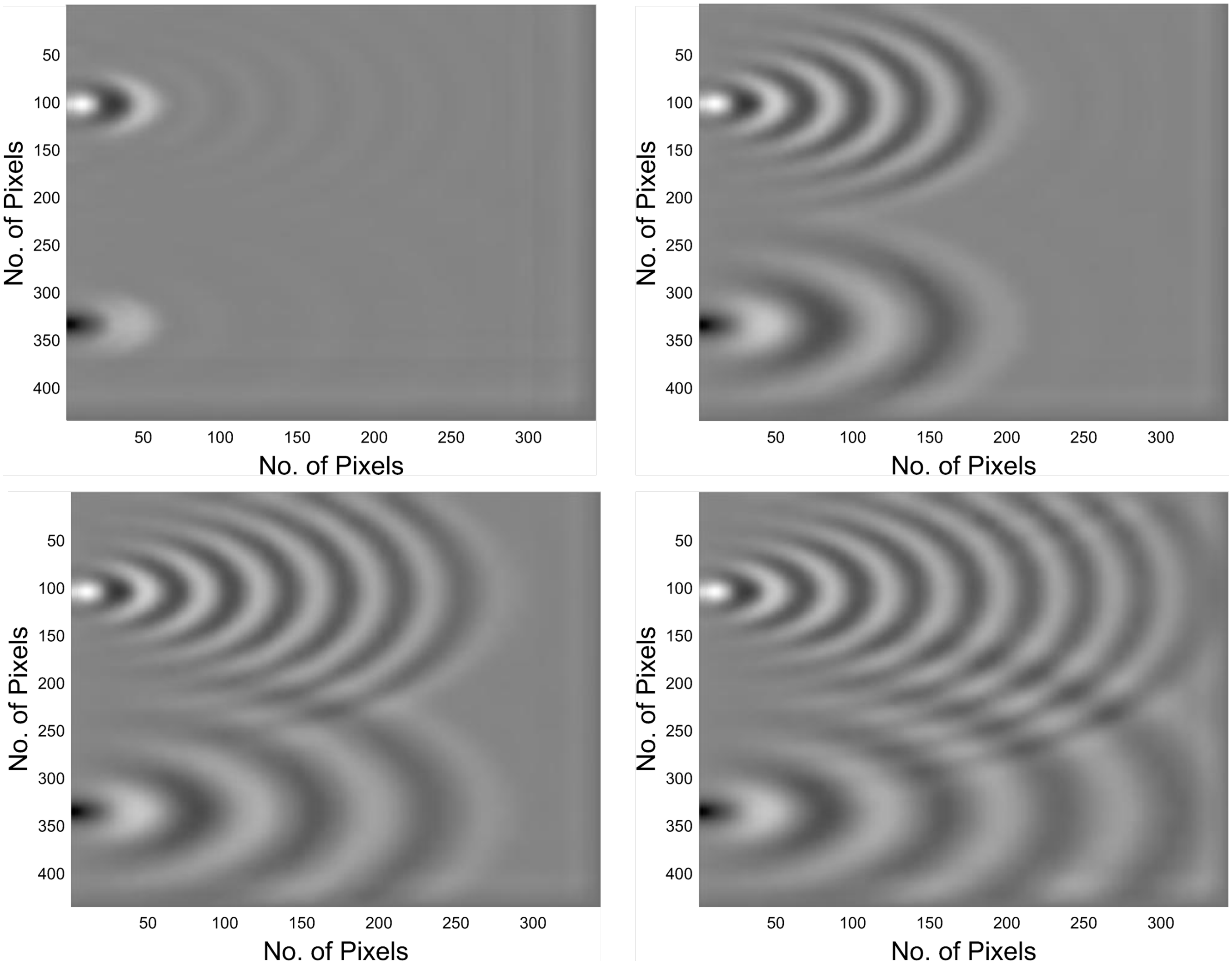

FIGURE 3: WAVE-INFORMED DECOMPOSITION BASED RECONSTRUCTION OF THE VIDEO OF WAVES EMERGING FROM TWO DIFFERENT DROPLETS OF DIFFERENT MASSES FALLING ONTO A WATER SURFACE

ACKNOWLEDGMENTS

This work is partially supported by NSF EECS-1839704 and NSF CISE-1747783.

REFERENCES

[1] Cawley, P. "Practical long range guided wave inspection – managing complexity." *Proc. of the Review of Progress in Quantitative Nondestructive Evaluation*, Vol. 22: pp. 22–40. 2003.

[2] Cawley, Peter. "Practical guided wave inspection and applications to structural health monitoring." *Proc. of the Australasian Congress on Applied Mechanics*: p. 10. 2007. Brisbane.

[3] Cawley, Peter. "Structural health monitoring: Closing the gap between research and industrial deployment." *Structural Health Monitoring* Vol. 17 No. 5 (2018): pp. 1225–1244.

[4] Davies, Jacob and Cawley, Peter. "The application of synthetic focusing for imaging crack-like defects in pipelines using guided waves." *IEEE Trans. Ultrason. Ferroelectr. Freq. Control* Vol. 56 No. 4 (2009): pp. 759–771.

[5] Liu, C, Harley, J, O'Donoughue, N, Ying, Y, Altschul, M H, Bergés, M, Garrett, J H, Greve, D W, Moura, J M F, Oppenheim, I J and Soibelman, L. "Robust change detection in highly dynamic guided wave signals with singular value decomposition." *2012 IEEE International Ultrasonics Symposium*: pp. 483–486. 2012. IEEE, Dresden.

[6] Ying, Yujie, Soibelman, Lucio, Harley, Joel, O'Donoughue, Nicholas, Garrett, James H, Jin, Yuanwei, Moura, José M F and Oppenheim, Irving J. "A data mining framework for pipeline monitoring using time reversal." *Proc. of SIAM Conference on Data Mining*. 2010. SIAM, Columbus, Ohio.

[7] Ying, Yujie, Garrett, James H, Jr., Harley, Joel, Oppenheim, Irving J, Shi, Jun and Soibelman, Lucio. "Damage Detection in Pipes under Changing Environmental Conditions Using Embedded Piezoelectric Transducers and Pattern Recognition Techniques." *J. Pipeline Syst. Eng. Pract.* Vol. 4 No. 1 (2013): pp. 17–23.

[8] Rizzo, Piervincenzo, Bartoli, Ivan, Marzani, Alessandro

and di Scalea, Francesco Lanza. "Defect Classification in Pipes by Neural Networks Using Multiple Guided Ultrasonic Wave Features Extracted After Wavelet Processing." *J. Pressure Vessel Technol.* Vol. 127 No. 3 (2005): pp. 294–303.

[9] Li, Jian and Rose, Joseph. "Angular-Profile Tuning of Guided Waves in Hollow Cylinders Using a Circumferential Phased Array." *IEEE Trans. Ultrason. Ferroelectr. Freq. Control* Vol. 49 No. 12 (2002): pp. 1720–1729.

[10] Chen, S, Cerda, F, Guo, J, Harley, J B, Shi, Q, Rizzo, P, Bielak, J, Garrett, J H and Kovacević, J. "Multiresolution classification with semi-supervised learning for indirect bridge structural health monitoring." *2013 IEEE International Conference on Acoustics, Speech and Signal Processing*: pp. 3412–3416. 2013. IEEE, Vancouver, BC.

[11] Holford, K M, Davies, A W, Pullin, R and Carter, D C. "Damage Location in Steel Bridges by Acoustic Emission." *J. Intell. Mater. Syst. Struct.* Vol. 12 No. 8 (2001): pp. 567–576.

[12] Chong, Ken P, Carino, Nicholas J and Washer, Glenn. "Health monitoring of civil infrastructures." *Smart Mater. Struct.* Vol. 12 No. 3 (2003): pp. 483–493.

[13] Baltazar, Arturo, Hernandez-Salazar, Cesar D and Manzanares-Martinez, Betsabe. "Study of wave propagation in a multiwire cable to determine structural damage." *NDT and E Int.* Vol. 43 No. 8 (2010): pp. 726–732.

[14] Rizzo, P. "Wave Propagation in Multi-Wire Strands by Wavelet-Based Laser Ultrasound." *Exp. Mech.* Vol. 44 No. 4 (2004): pp. 407–415.

[15] Rizzo, P and Lanza di Scalea, F. "Acoustic emission monitoring of carbon-fiber-reinforced-polymer bridge stay cables in large-scale testing." *Exp. Mech.* Vol. 41 No. 3 (2001): pp. 282–290.

[16] Ihn, Jeong-Beom and Chang, Fu-Kuo. "Pitch-catch Active Sensing Methods in Structural Health Monitoring for Aircraft Structures." *Structural Health Monitoring* Vol. 7 No. 1 (2008): pp. 5–19.

[17] Worden, K, Manson, G and Allman, D. "Experimental Validation of a Structural Health Monitoring Methodology: Part I. Novelty Detection on a Laboratory Structure." *J. Sound Vib.* Vol. 259 No. 2 (2003): pp. 323–343.

[18] Leckey, Cara A C, Rogge, Matthew D and Raymond Parker, F. "Guided waves in anisotropic and quasi-isotropic aerospace composites: three-dimensional simulation and experiment." *Ultrasonics* Vol. 54 No. 1 (2014): pp. 385–394.

[19] Staszewski, W J, Mahzan, S and Traynor, R. "Health monitoring of aerospace composite structures – Active and passive approach." *Compos. Sci. Technol.* Vol. 69 No. 11-12 (2009): pp. 1678–1685.

[20] Qiu, Lei, Yuan, Shenfang, Zhang, Xiaoyue and Wang, Yu. "A time reversal focusing based impact imaging method and its evaluation on complex composite structures." *Smart Mater. Struct.* Vol. 20 No. 10 (2011): p. 105014.

[21] Salamone, Salvatore, Bartoli, Ivan, Lanza Di Scalea, Francesco and Coccia, Stefano. "Guided-wave Health Monitoring of Aircraft Composite Panels under Changing Temperature." *J. Intell. Mater. Syst. Struct.* Vol. 20 No. 9 (2009): pp. 1079–1090.

[22] Castellini, P., Martarelli, M. and Tomasini, E.P. "Laser Doppler Vibrometry: Development of advanced solutions answering to technology's needs." *Mechanical Systems and Signal Processing* Vol. 20 No. 6 (2006): pp. 1265–1285. Special Issue: Laser Doppler Vibrometry.

[23] Raissi, M., Perdikaris, P. and Karniadakis, G.E. "Physics-informed neural networks: A deep learning framework for solving forward and inverse problems involving nonlinear partial differential equations." *Journal of Computational Physics* Vol. 378 (2019): pp. 686–707.

[24] Shukla, Khemraj, Di Leoni, Patricio Clark, Blackshire, James, Sparkman, Daniel and Karniadakis, George Em. "Physics-informed neural network for ultrasound nondestructive quantification of surface breaking cracks." *Journal of Nondestructive Evaluation* Vol. 39 (2020): pp. 1–20.

[25] Yu, Yang, Wang, Chaoyue, Gu, Xiaoyu and Li, Jianchun. "A novel deep learning-based method for damage identification of smart building structures." *Structural Health Monitoring* Vol. 18 No. 1 (2019): pp. 143–163.

[26] Moseley, Ben, Markham, Andrew and Nissen-Meyer, Tarje. "Solving the wave equation with physics-informed deep learning." *arXiv preprint arXiv:2006.11894* (2020).

[27] Rasht-Behesht, Majid, Huber, Christian, Shukla, Khemraj and Karniadakis, George Em. "Physics-Informed Neural Networks (PINNs) for Wave Propagation and Full Waveform Inversions." *Journal of Geophysical Research: Solid Earth* Vol. 127 No. 5 (2022): p. e2021JB023120.

[28] Tetali, Harsha Vardhan, Alguri, K Supreet and Harley, Joel B. "Wave Physics Informed Dictionary Learning In One Dimension." *2019 IEEE 29th International Workshop on Machine Learning for Signal Processing (MLSP)*: pp. 1–6. 2019. IEEE.

[29] Tetali, Harsha Vardhan, Harley, Joel B and Haeffele, Benjamin D. "Wave-Informed Matrix Factorization with Global Optimality Guarantees." *arXiv preprint arXiv:2107.09144* (2021).

[30] Tetali, Harsha Vardhan and Harley, Joel. "A physics-informed machine learning based dispersion curve estimation for non-homogeneous media." *The Journal of the Acoustical Society of America* Vol. 152 No. 4 (2022): pp. A239–A239.

[31] Taylor, Brook. *Methodus incrementorum directa & inversa*. Inny (1717).

[32] Robinson, Enders A. "History of the wave equation and transforms in engineering." *Review of Progress in Quantitative Nondestructive Evaluation* (1990): pp. 29–35.

[33] Silva, Moisés, Figueiredo, Eloi, Costa, João C.W.A. and Mascareñas, David. "Spatio-temporal decomposition of 2D travelling waves from video measurements." *Mechanical Systems and Signal Processing* Vol. 139 (2020): p. 106599.

[34] Srebro, Nathan and Shraibman, Adi. "Rank, trace-norm and max-norm." *Proc. of the International Conference on Computational Learning Theory*: pp. 545–560. 2005. Springer.

[35] Recht, Benjamin, Fazel, Maryam and Parrilo, Pablo A. "Guaranteed minimum-rank solutions of linear matrix equations via nuclear norm minimization." *SIAM review* Vol. 52 No. 3 (2010): pp. 471–501.

[36] Haeffele, Benjamin, Young, Eric and Vidal, Rene. "Structured low-rank matrix factorization: Optimality, algorithm, and applications to image processing." *Proc. of the International Conference on Machine Learning*: pp. 2007–2015. 2014.

[37] Haeffele, Benjamin David and Vidal, René. "Structured low-rank matrix factorization: Global optimality, algorithms, and applications." *IEEE Transactions on Pattern Analysis and Machine Intelligence* Vol. 42 No. 6 (2019).